Supporting Information

Carbon quantum dot–mediated Fe_{11} polyoxometalate enrichment for accelerated photocatalytic H_2 evolution in a $Zn_{0.5}Cd_{0.5}S$ system

Khalid Umer [a], Xiao Fang [a], Khuram Hasnain [a], Hira Shahid [a], Weize Sun [a], Chenyu Shi [a], Junhan Xie [a], Baochun Ma [a], Yong Ding [a, b] *

[a] *State Key Laboratory of Natural Product Chemistry, Key Laboratory of Advanced Catalysis of Gansu Province, College of Chemistry and Chemical Engineering, Lanzhou University, 222 Tianshui South Road, Lanzhou 730000, China.*

[b] *State Key Laboratory of Low Carbon Catalysis and Carbon Dioxide Utilization; State Key Laboratory for Oxo Synthesis and Selective Oxidation, Lanzhou Institute of Chemical Physics, Chinese Academy of Sciences, Lanzhou 730000, China.*

Corresponding author's E-mail:

dingyong1@lzu.edu.cn (Y. Ding)

1. Materials

The reagents utilized in this research were selected based on their exceptional purity and consistent quality, thereby guaranteeing the dependability and replicability of our experimental findings. Sodium tungstate dihydrate ($Na_2WO_4 \cdot 2H_2O$), antimony oxide (Sb_2O_3) and hydrochloric acid (HCl) were obtained from Shanghai Macklin Biochemical Co., Ltd. Iron(III) chloride ($FeCl_3$), zinc acetate dihydrate ($Zn(CH_3COO)_2 \cdot 2H_2O$), cadmium acetate dihydrate ($Cd(CH_3COO)_2 \cdot 2H_2O$) and sodium sulfide nonahydrate ($Na_2S \cdot 9H_2O$) were acquired from Shanghai Chemical Reagent Co., Ltd.

1.1 Synthesis of CdS nanorods

CdS nanorods were prepared via hydrothermal synthesis procedure according to a literature [1]. In a typical run, 5 g $Cd(NO_3)_2 \cdot 4H_2O$ and 3.7 g $CS(NH_2)_2$ were dissolved in 60 mL ethylenediamine under continuous stirring. After continuous stirring for 1 h, the obtained homogenous mixture was transferred into a 100 mL Teflon-lined stainless-steel autoclave and hydrothermally treated at 180 °C for 24 h. After the autoclave was cooled down to room temperature, a vivid yellow precipitates were synthesized. The precipitates were collected by centrifugation and washed thoroughly with deionized water. Then the final products were dried at 60 °C overnight in a vacuum oven and stored for further use .

1.2 Synthesis of $Mn_xCd_{1-x}S$

The $Mn_xCd_{1-x}S$ was synthesized by following the method reported in the literature [2] by hydrothermal method with some modifications, 0.49 g of manganese acetate tetrahydrate ($Mn(CH_3COO)_2 \cdot 4H_2O$), and 2.13 g of cadmium acetate dihydrate ($Cd(CH_3COO)_2 \cdot 2H_2O$), were

dissolved in 50 mL ultrapure water with continuous stirring for 10 minutes and then 2.4 g of sodium sulfide ($Na_2S·9H_2O$) was added to the solution and kept stirring until dissolved. The solution was poured into a 100 mL Teflon-lined autoclave and put into the heating furnace at 160 °C for 24 hours; after naturally cooling at room temperature, the solution was centrifuged to collect the product named $Mn_{0.2}Cd_{0.8}S$ by washing several times with deionized water and ethanol and dried at 70° C for 6 hours.

1.3 Synthesis of SnS_2, Zn-SnS_2 and Mn-SnS_2

In a typical synthesis procedure reported in literature [3], 1 mmol $SnCl_2·2H_2O$, 2 mmol TAA and 0.5 g PVP were added into 30 mL TEG with vigorous magnetic stirring at room temperature. Then the clear solution was transferred into a 50 mL Teflon-lined stainless-steel autoclave, heated at 220 °C for 12 h, and cooled to room temperature naturally. The resultant product was centrifuged at 10 000 rpm for 8 min and washed several times with ethanol. Finally, the yellow SnS_2 powder was obtained after dried at 60 °C overnight. The Zn-SnS_2 and Mn-SnS_2 was synthesized by adding specific amount of $Zn(CH_3COO)_2$ and $MnCl_2·4H_2O$ in above mentioned solution respectively by adopting same procedure.

1.4 Synthesis of MoS_2, Zn-MoS_2 and Mn-MoS_2

Synthesis of MoS_2 was carried out by following the method reported in literature [4]. Usually, a mixture of 1.24 g of ammonium heptamolybdate tetrahydrate ($(NH_4)_6Mo_7O_{24}·4H_2O$) and 2.28 g of thiourea was dissolved in 35 mL of deionized water with strong stirring in a beaker. The resulting uniform solution was then placed into a 50-milliliter Teflon-lined stainless-steel autoclave. The autoclave was heated to a temperature of 200° C for a duration of 12 h and then cooled to an ambient temperature. The black sediment collected was rinsed with deionized water and absolute ethanol many times, and then dried at a temperature of 60° C for the duration of one night. The Zn-MoS_2 and Mn-MoS_2 was synthesized by adding specific amount of $Zn(CH_3COO)_2$

and $MnCl_2 \cdot 4H_2O$ in above mentioned solution respectively by adopting same procedure.

1.5 Characterization of materials

All chemicals were analytical, purchased from commercial sources and were utilized without any further purification. Pure water (18.2 MΩ cm, TOC < 3 ppb) was produced by Molecular Lab Water Purifier. IR spectra (2-4 wt% samples in KBr pellets) were recorded on a Bruker VERTEX 70v FT-IR spectrometer. X-ray diffraction (XRD) spectra were measured by Rigaku D/MAX 2400 diffractometer (Japan) with Cu Kα radiation (k = 1.5418 Å) operating at 40 kV and 40 mA. Photoluminescence (PL) spectra were performed on FLS920 fluorescence spectrometer (Edinburgh Instruments). High resolution X-ray photoelectron spectroscopy (XPS) data were measured by Axis Supra and the binding energy of all the elements were corrected by the C 1s peak (284.8 eV). The optical properties of the solid samples were measured by Shimadzu UV-2600 UV−vis diffuse reflectance spectrophotometer. The surface morphology of the samples was characterized by a field emission scanning electron microscope (SEM, JSM-6701F, Japan) and transmission electron microscopy (TEM, Talos F200S, America). The H_2 amount was detected by gas chromatography (GC) analysis.

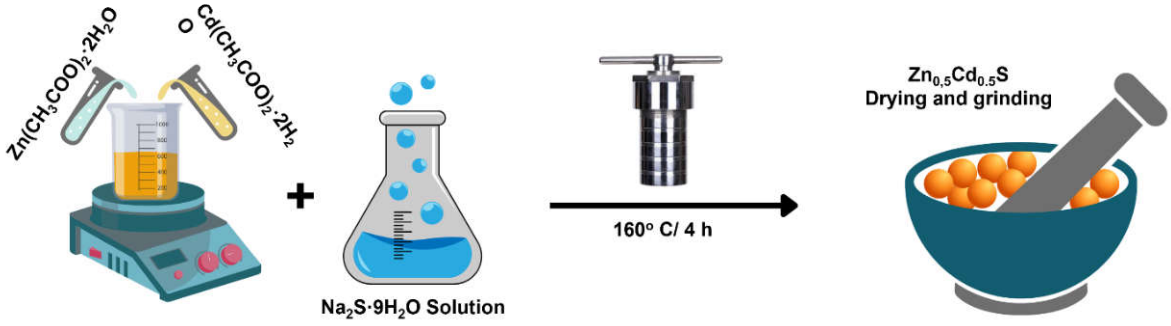

Figure S1 Synthesis scheme of $Zn_{0.5}Cd_{0.5}S$.

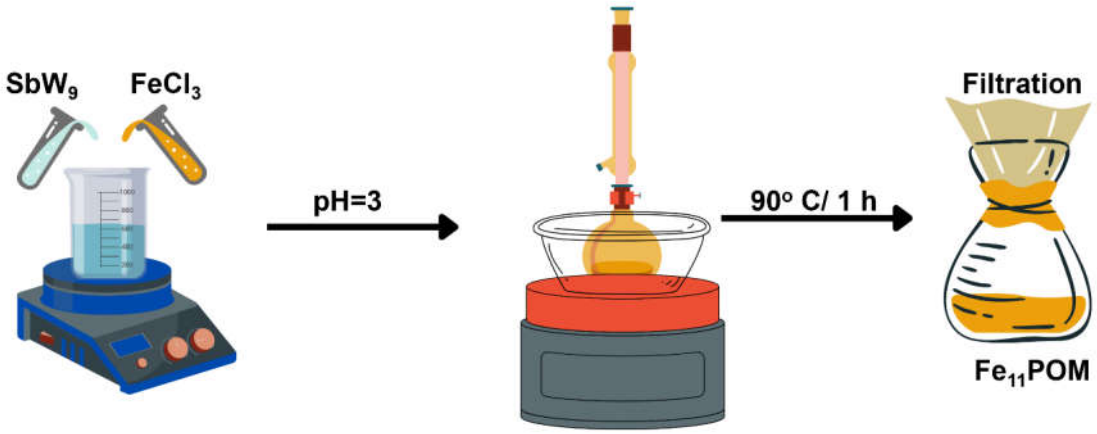

Figure S2 Synthesis scheme of $Fe_{11}POM$.

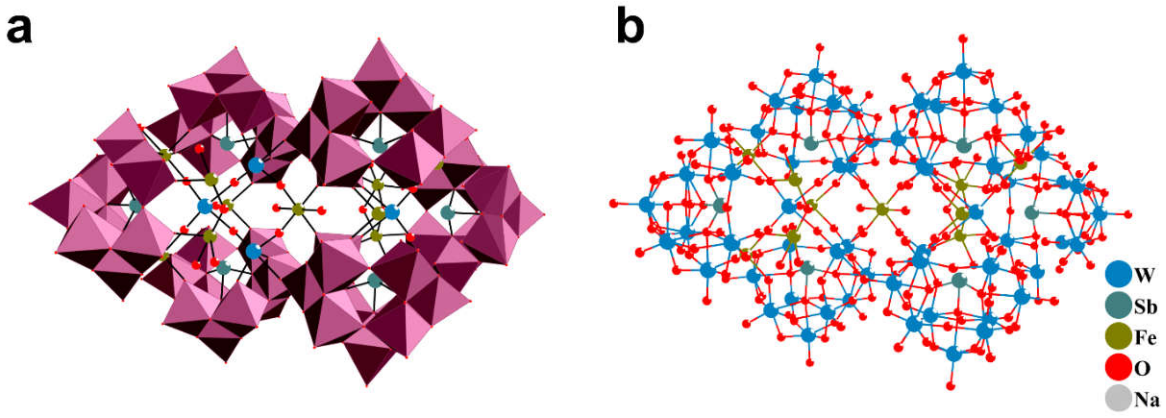

Figure S3 (a) Combined polyhedral/ball-and-stick representation of $Fe_{11}POM$, color scheme: [α-$SbW_9O_{33}]^{9-}$ polyhedra (crimson red), W (blue), Fe (brownish), O/H_2O/OH (red), Sb green and b) simple ball and stick structure of $Fe_{11}POM$.

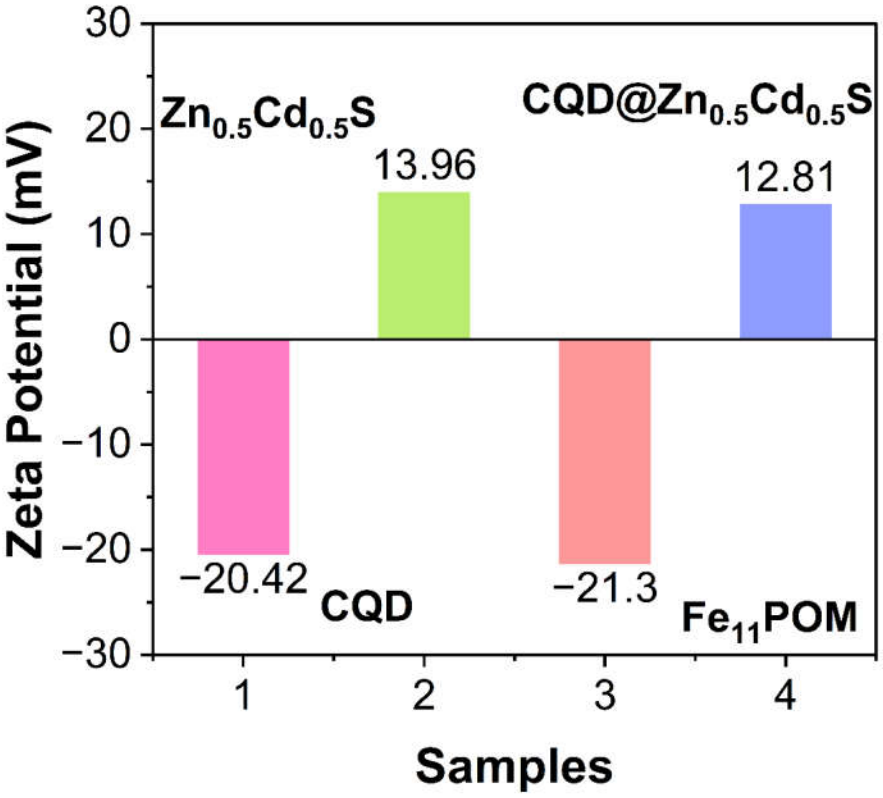

Figure S4 The zeta potential analysis of CQD, $Zn_{0.5}Cd_{0.5}S$, CQD@$Zn_{0.5}Cd_{0.5}S$ and Fe_{11}POM.

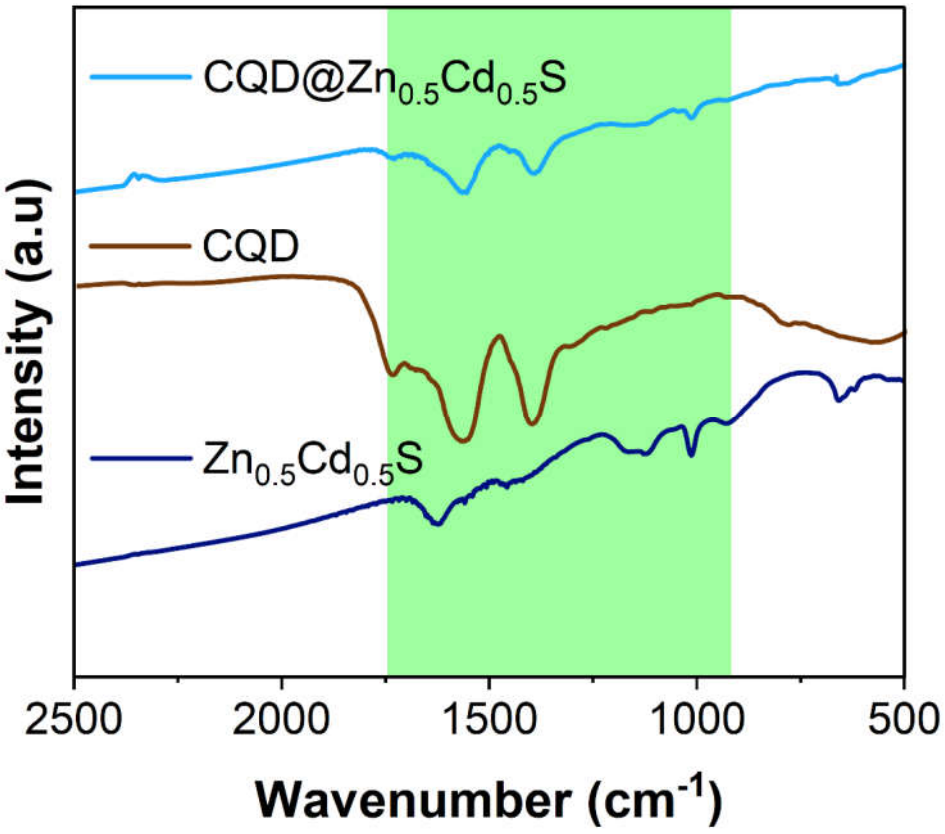

Figure S5 FTIR spectra of $Zn_{0.5}Cd_{0.5}S$, CQD and CQD@ $Zn_{0.5}Cd_{0.5}S$.

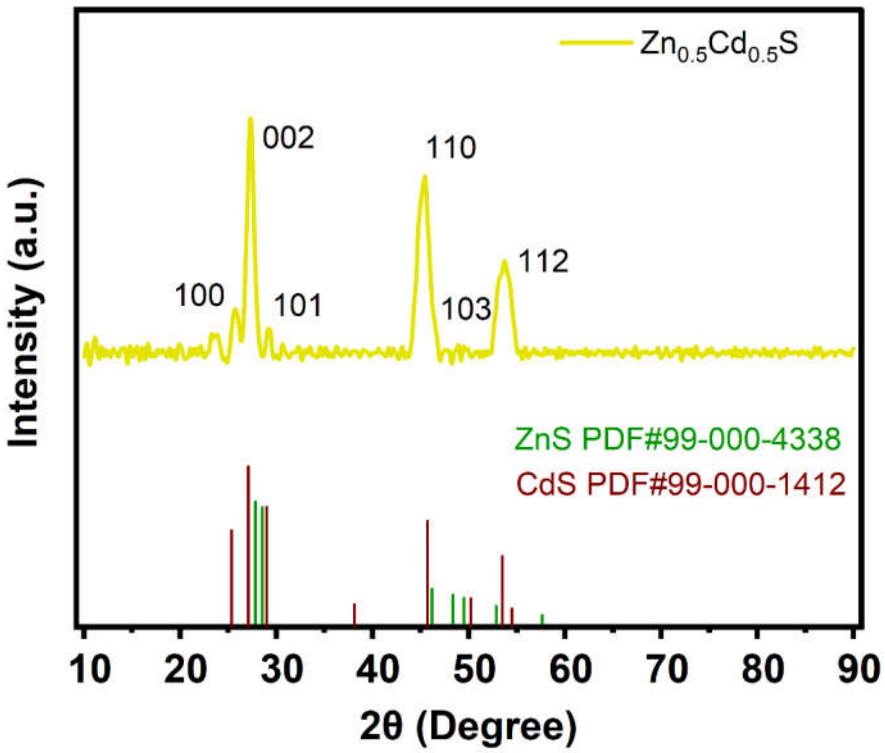

Figure S6 XRD pattern for $Zn_{0.5}Cd_{0.5}S$ compared with ZnS PDF#99-000-4338 and CdS PDF#99-000-1412.

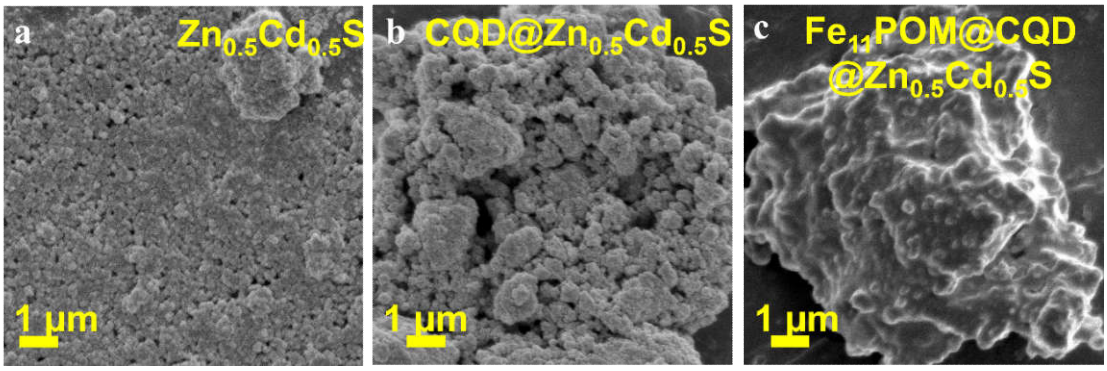

Figure S7 Scanning electron microscopy (SEM) images of (a) $Zn_{0.5}Cd_{0.5}S$; (b) CQD@ $Zn_{0.5}Cd_{0.5}S$; (c) $Fe_{11}POM@CQD@Zn_{0.5}Cd_{0.5}S$.

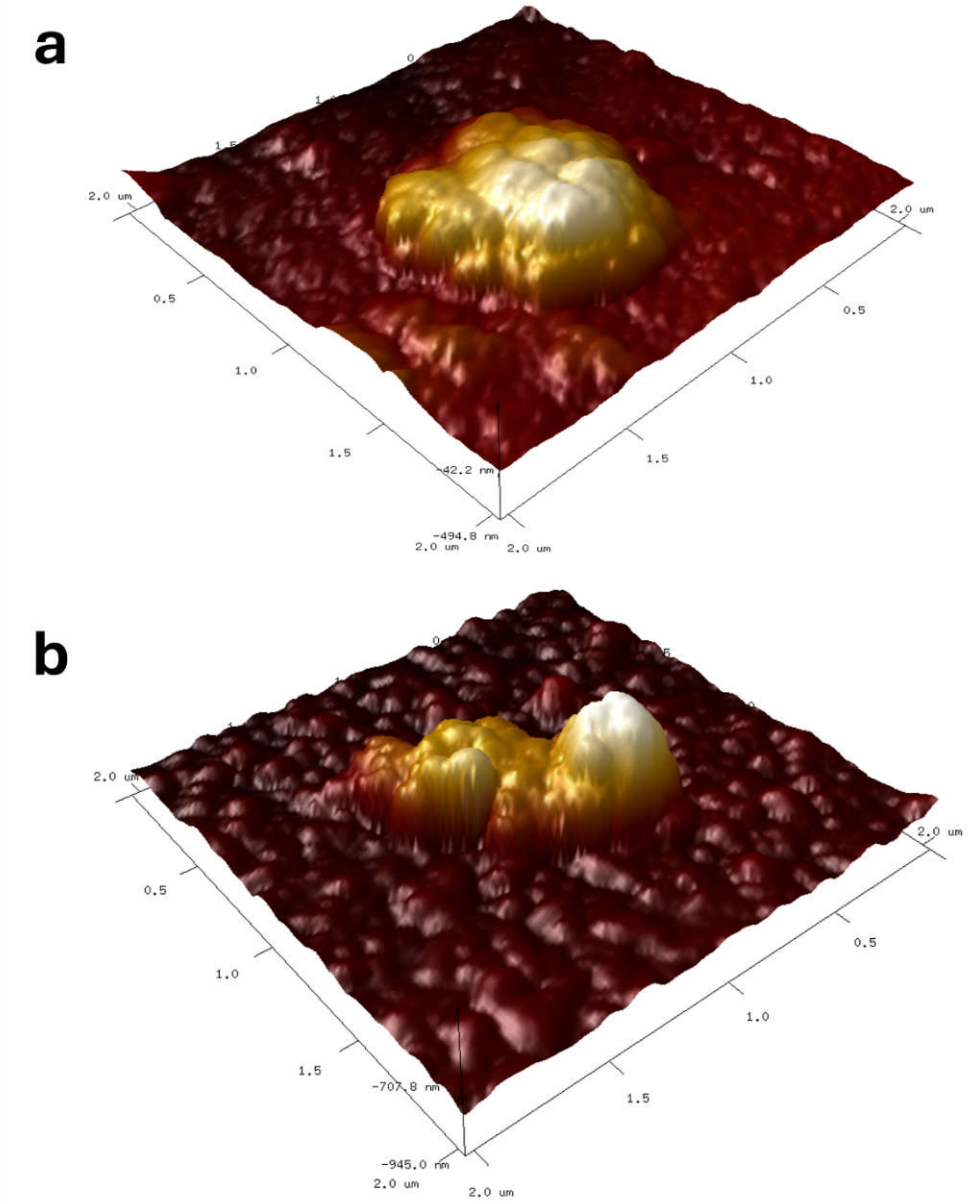

Fig S8 Three-dimensional Kelvin Probe Force Microscopy (KPFM) surface potential maps of (a) $Zn_{0.5}Cd_{0.5}S$ and (b) Fe_{11}POM@CQD@$Zn_{0.5}Cd_{0.5}S$ composites.

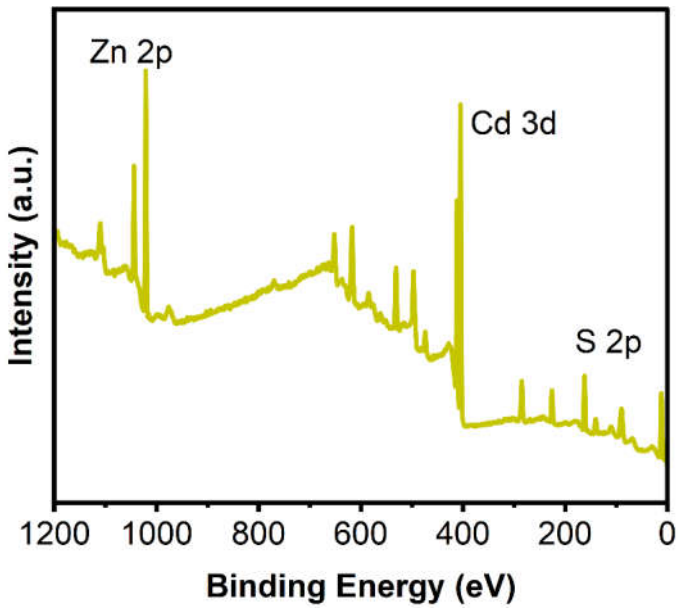

Figure S9 XPS survey for $Zn_{0.5}Cd_{0.5}S$.

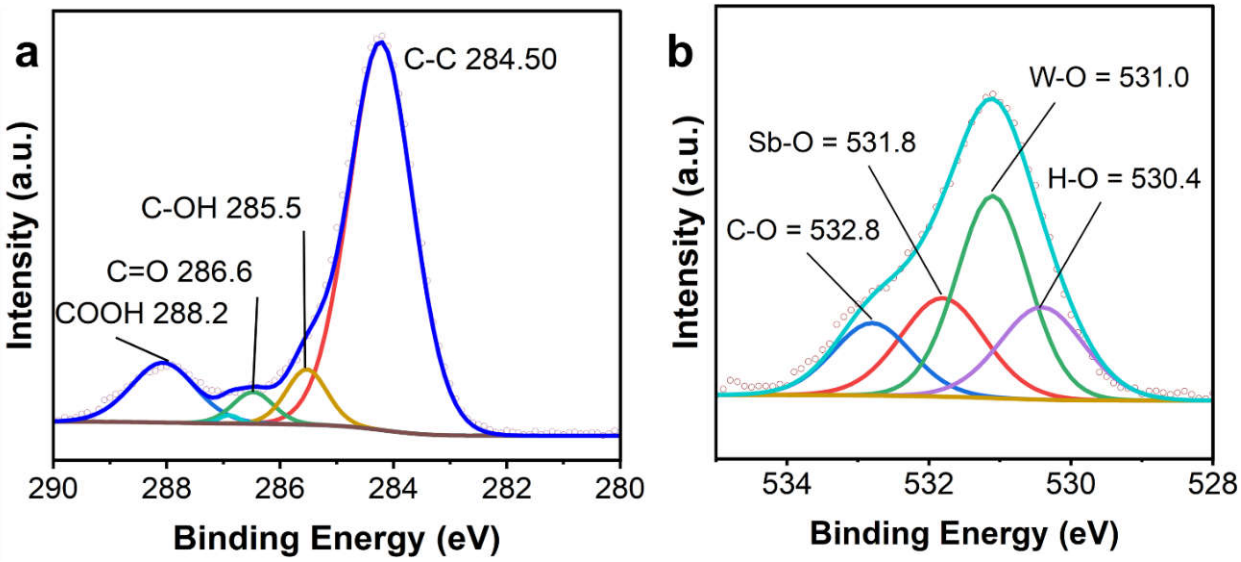

Figure S10 XPS spectra of (a) C 1s; (b) O 1s in Fe_{11}POM@CQD@$Zn_{0.5}Cd_{0.5}S$.

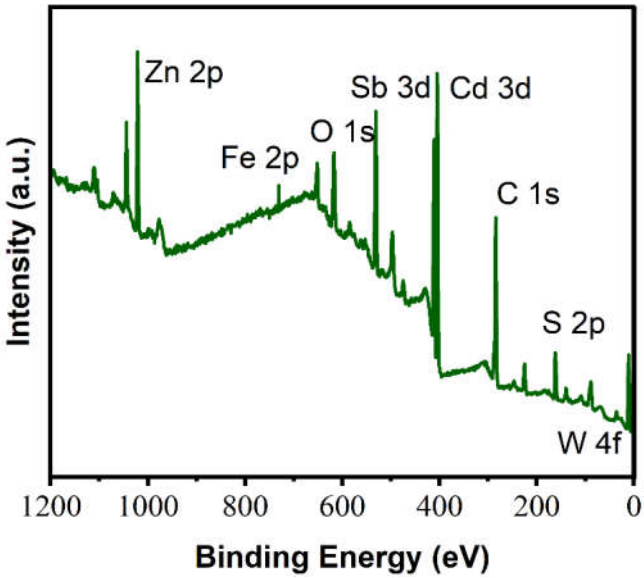

Figure S11 XPS survey for Fe_{11}POM@CQD@$Zn_{0.5}Cd_{0.5}S$.

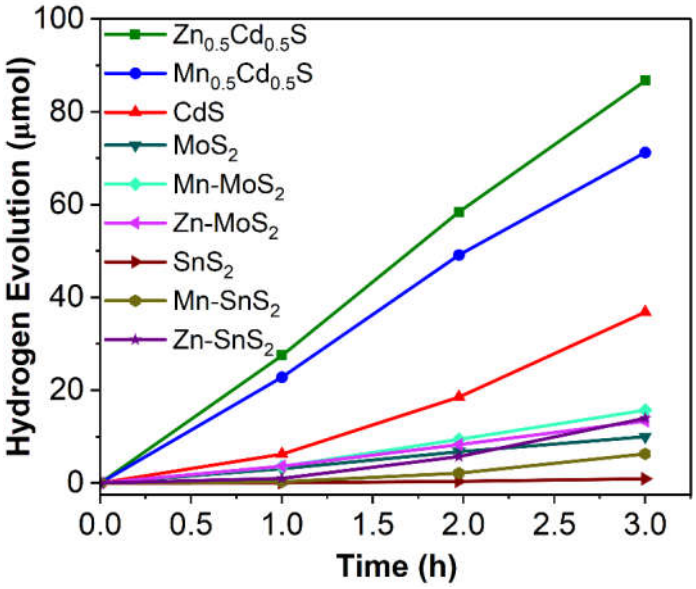

Figure S12 Photocatalytic hydrogen evolution activity for 3 hours cycle using CdS, $Mn_{0.5}Cd_{0.5}S$, $Zn_{0.5}Cd_{0.5}S$, MoS_2, Mn-MoS_2, Zn-MoS_2, SnS_2, Mn-SnS_2, and Zn-SnS_2 catalysts.

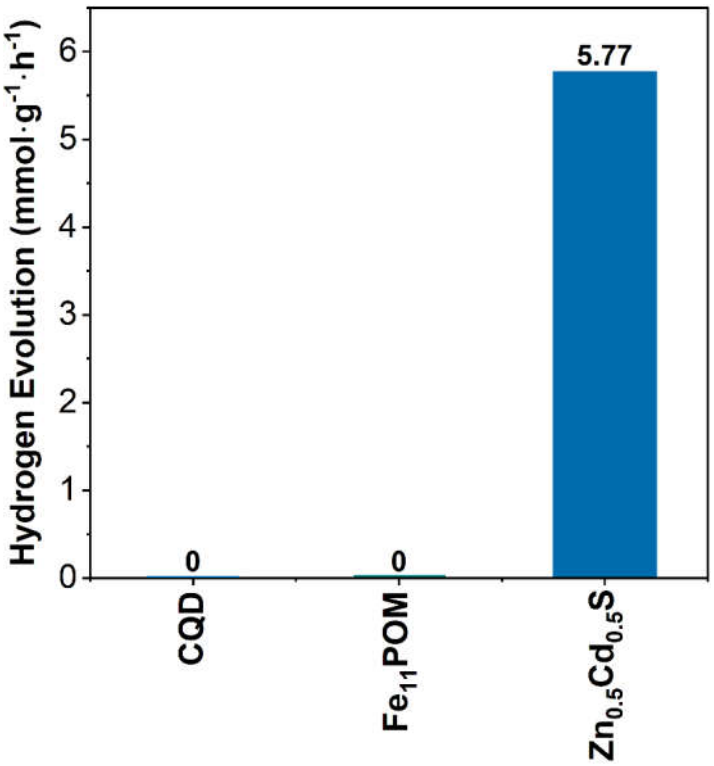

Figure S13 Photocatalytic hydrogen evolution activity test under controlled conditions using pure catalysts.

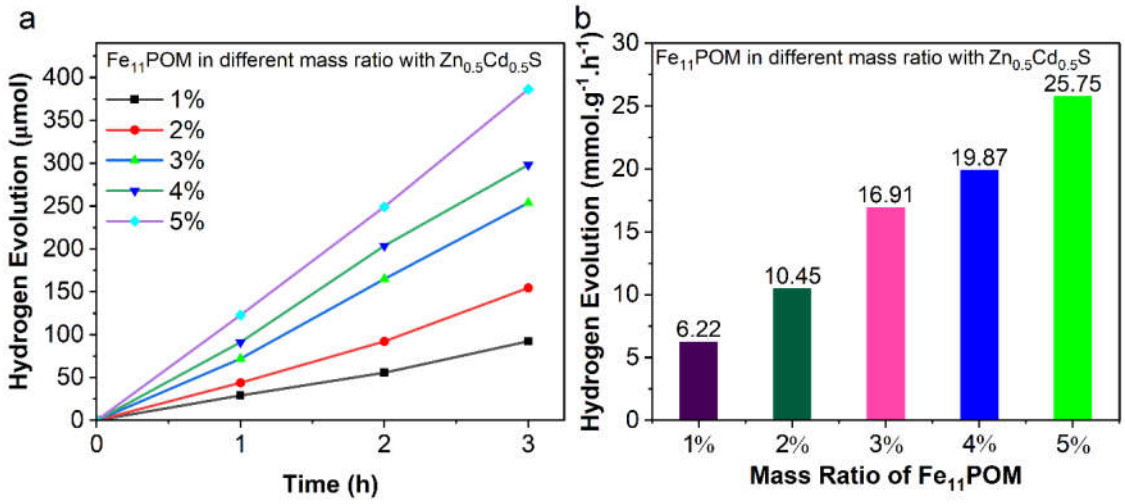

Figure S14 (a,b) Photocatalytic hydrogen evolution activity test using $Fe_{11}POM$ in different ratios with $Zn_{0.5}Cd_{0.5}S$.

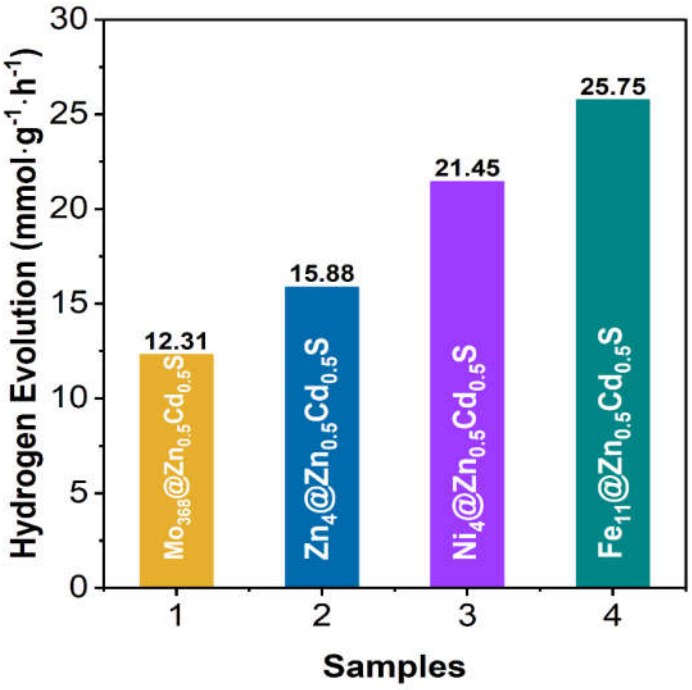

Fig. S15 Photocatalytic activity of $Zn_{0.5}Cd_{0.5}S$ in combination with different POMs.

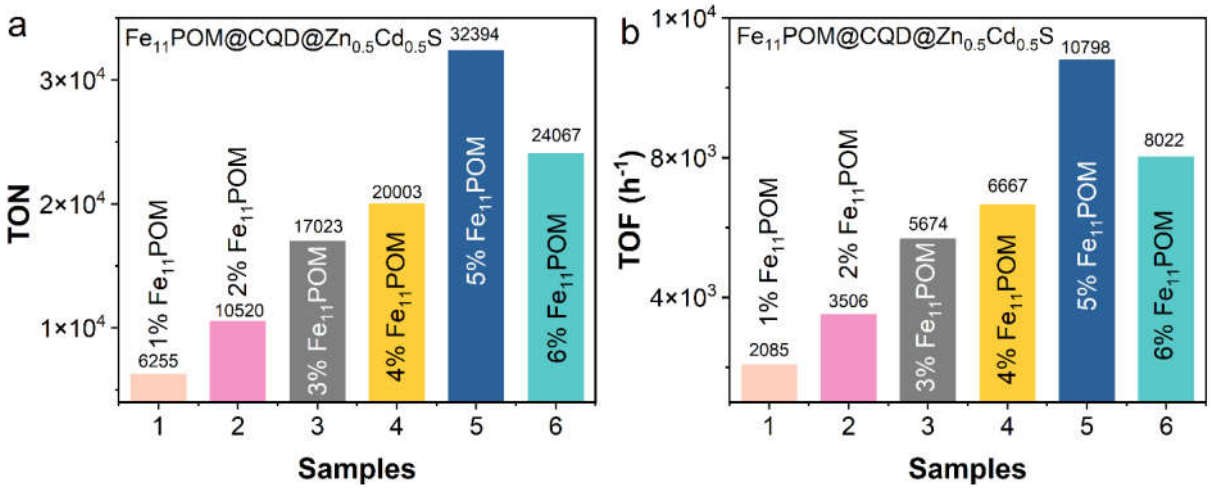

Figure S16 (a) Turn over number (TON); (b) Turn over frequency (TOF) for $Fe_{11}POM@CQD@Zn_{0.5}Cd_{0.5}S$ with different mass ratios of $Fe_{11}POM$.

The TON of photocatalytic reaction was calculated with the following formula.

$$\text{TON} = \frac{Moles\ of\ H_2\ evolved}{Moles\ of\ Fe_{11}POM\ loaded\ on\ catalyst}$$

The TOF of photocatalytic reaction was measured with the formula given below.

$$\text{TOF} = \frac{TON}{Time\ of\ reaction\ (h)}$$

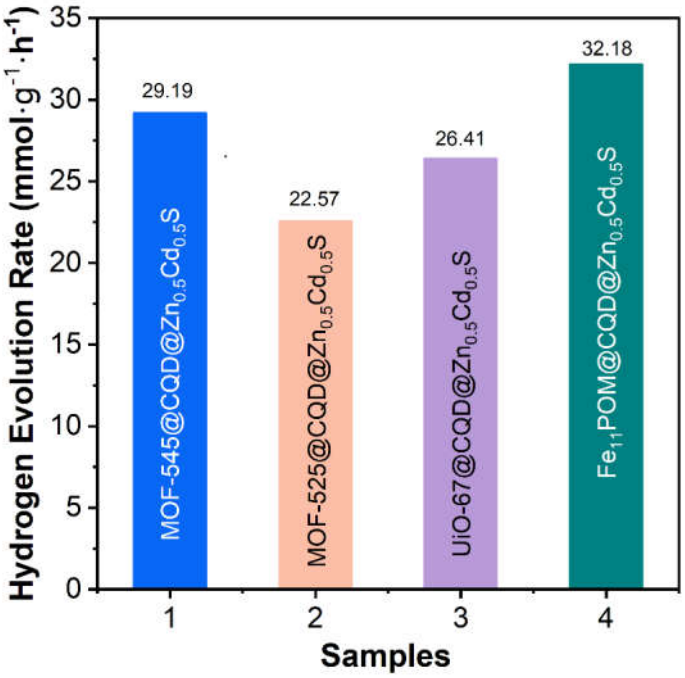

Figure S17 Photocatalytic activity comparison of MOF-545@CQD@$Zn_{0.5}Cd_{0.5}S$, MOF-525@CQD@$Zn_{0.5}Cd_{0.5}S$, and UiO-67@CQD@$Zn_{0.5}Cd_{0.5}S$ with the Fe_{11}POM@CQD@$Zn_{0.5}Cd_{0.5}S$.

Table S1: Comparison of different POMs, Nobel metals and non-POM based system.

Catalyst	Sacrificial agent	Hydrogen Evolution Rate $mmol \cdot g^{-1} \cdot h^{-1}$	References in SI
$Fe_{11}POM@CQD@Zn_{0.5}Cd_{0.5}S$	Lactic Acid	32.18	This work
$MOF\text{-}545@CQD@Zn_{0.5}Cd_{0.5}S$	Lactic Acid	29.19	This work
$MOF\text{-}525@CQD@Zn_{0.5}Cd_{0.5}S$	Lactic Acid	22.57	This work
$UiO\text{-}67@CQD@Zn_{0.5}Cd_{0.5}S$	Lactic Acid	26.41	This work
Ni_4P_2-CQDs@CdS	No	0.145	[1]
$[Co]_{x\%}\text{-}[HC{\equiv}C]_{(17-x)\%}$-TAPD COFs	EtOH	0.038	[5]
Pt/ DRPS-$ZnIn_2S_4$	Methanol	26.84	[6]
$BaTiO_3@Zn0.5Cd_{0.5}S$	Methanol	1.19	[7]
P-gCN/PMA_x	Triethanolamine	0.625	[8]
$HPM@ZnIn_2S_4$	Benzyl Alcohol	10.6	[9]
$Pt/Zn_{0.2}Cd_{0.8}S/Cs_3PW_{12}O_{40}$	Lactic Acid	10.4	[10]
CdS/Ni_3-POM	Na_2SO_3/ Na_2S	10.14	[11]
$K_7[Co^{III}Co^{II}(H_2O)W_{11}O_{39}]$	TEOA	13.39	[12]

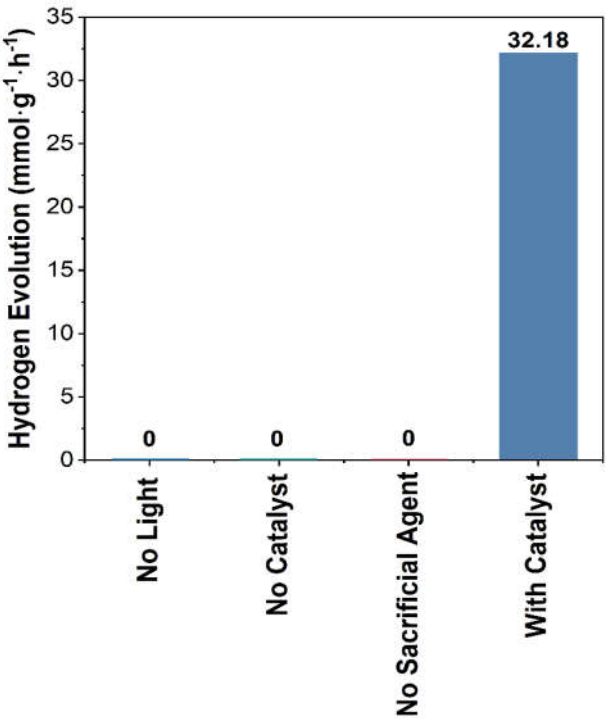

Figure S18 Photocatalytic hydrogen evolution activity test under controlled conditions.

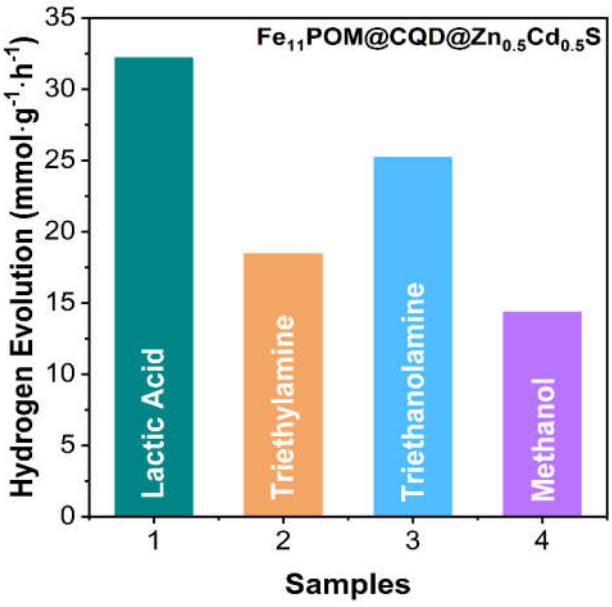

Figure S19 Photocatalytic activity of Fe_{11}POM@CQD@$Zn_{0.5}Cd_{0.5}S$ using different sacrificial agents.

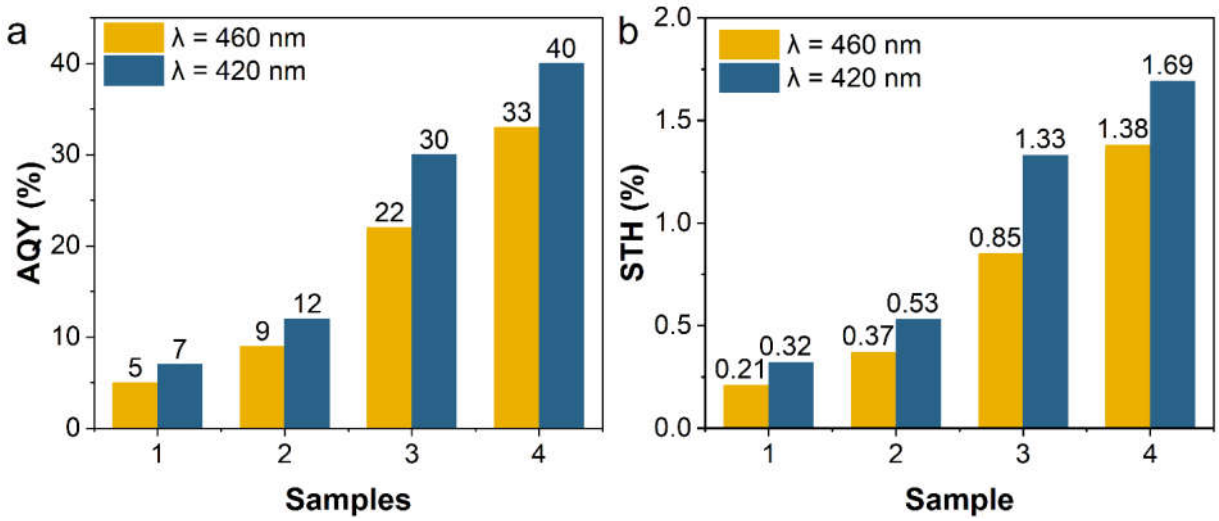

Figure S20 (a) Apparent quantum yield (AQY); (b) The Solar-to-hydrogen (STH) conversion efficiency for $Zn_{0.5}Cd_{0.5}S$ (1), CQD@$Zn_{0.5}Cd_{0.5}S$ (2), Fe_{11}POM@$Zn_{0.5}Cd_{0.5}S$ (3) and Fe_{11}POM@CQD@$Zn_{0.5}Cd_{0.5}S$ (4).

The AQY% was calculated by using the formula.

$$\text{AQY}(\%) = \frac{2 \times Number\ of\ H_2\ molecules\ evolved}{Number\ of\ incident\ photons} \times 100$$

Number of H_2 molecules evolved = Moles of Hydrogen Evolved (n_{H_2}) × N_A

$$\text{Number of incident photons} = \frac{E_{total}}{E_{photon}}$$

$$E_{total} = PSt$$

where P (Wm^{-2}) is power density of incident light, S (m^2) is the area of irradiation and t (s) is time of photocatalytic reaction.

$$E_{photon} = \frac{hc}{\lambda_{inc}}$$

where h is Panck's constant 6.626×10^{-34} J·s, c is speed of light 3×10^{8} ms^{-1} and λ_{inc} is wavelength of incident light. So, the number of incident photons will be,

$$\text{Number of incident photons} = \frac{PS\lambda_{inc}t}{\text{hc}}$$

$$\text{AQY}(\%) = \frac{2n_{H_2} \times N_A \times \text{hc}}{PS\lambda_{inc}t} \times 100$$

The STH% of photocatalytic system was measured with the help of formula [1].

$$\text{STH}\ (\%) = \left(\frac{Produced\ H_2\ (mmol/s) \times \Delta G}{P_{inc}(mWcm^{-2}) \times A\ (cm)^2}\right) \times 100$$

where ΔG is Gibbes free energy constant which is 237 $KJmol^{-1}$ at room temperature, P_{inc} is energy density of sunlight and A is area of incidence.

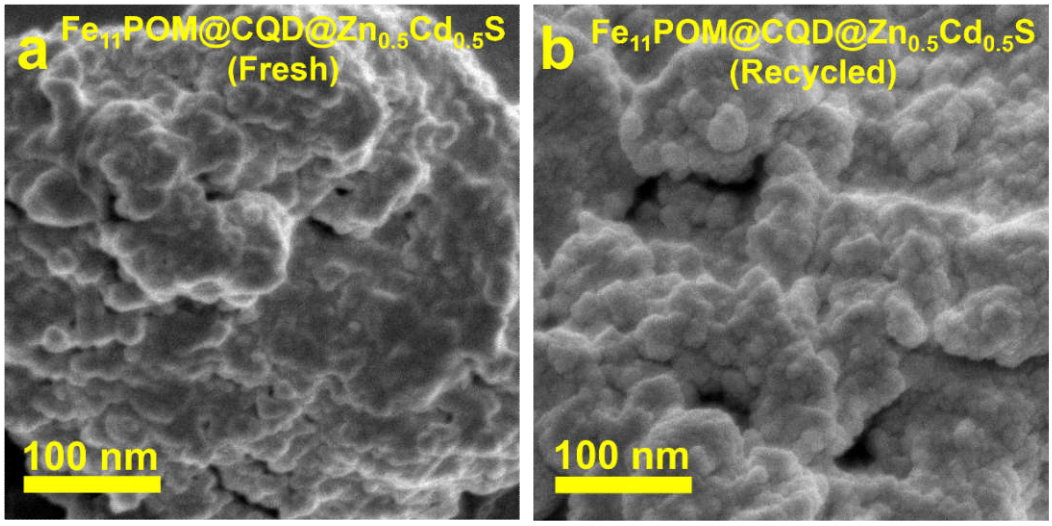

Figure S21 (a, b) SEM analysis of fresh and recycled $Fe_{11}POM@CQD@Zn_{0.5}Cd_{0.5}S$.

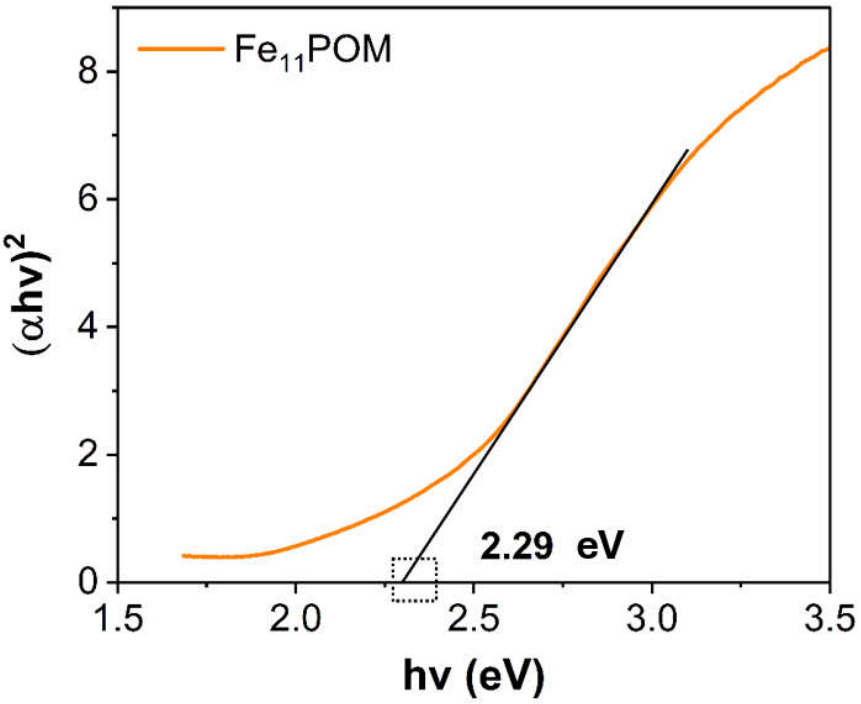

Figure S22 Tauc plot to calculate band gap of $Fe_{11}POM$.

References

1. Dong, Y., Han, Q., Hu, Q., Xu, C., Dong, C., Peng, Y., Ding, Y., and Lan, Y., *Appl. Catal. B: Environ. Energy*, 2021, 293, 120214.
2. Umer, K., Li, B., Shahid, H., Ali, S., Hasnain, K., Huang, J., Yang, X., Fang, X., Hu, C., Wu, J., Li, Z., and Ding, Y., *Appl. Catal. B: Environ. Energy*, 2025, 373, 125357.
3. Yu, J., Xu, C.-Y., Ma, F.-X., Hu, S.-P., Zhang, Y.-W., and Zhen, L., *ACS Appl. Mater. Interfaces*, 2014, 6, 22370-22377.
4. Umer, K., Hasnain, K., Li, B., Shahid, H., Fang, X., Zhang, X., Ma, B., and Ding, Y., *Catal. Today*, 2025, 459, 115438.
5. Wang, S., Wu, T., Wu, S., Guo, J., He, T., Wu, Y., Yuan, W., Zhang, Z., Hua, Y., and Zhao, Y., *Angew. Chem. Int. Ed.*, 2023, 62, e202311082.
6. Ruan, X., Meng, D., Huang, C., Xu, M., Jiao, D., Cheng, H., Cui, Y., Li, Z., Ba, K., Xie, T., Zhang, L., Zhang, W., Leng, J., Jin, S., Ravi, S.K., Jiang, Z., Zheng, W., Cui, X., and Yu, J., *Adv. Mater.*, 2024, 36, 2309199.
7. Pan, C., Huang, K., Zhi, Z., Yang, Y., Zhang, H., Xie, Y., Zhang, C., Liu, Y., Chen, M., Wang, Z., Jiang, Z., and Cao, D., *Adv. Energy Mater.*, 2025, 16, 2405708.
8. Djoko T, S.Y., Njoyim T, E., Nguyen, A.D., Yang, J., Küçükkeçeci, H., Kutorglo, E.M., Radhakrishnan, B., Schwarzburg, K., Huseyinova, S., Das, P., Tasbihi, M., Schwarze, M., Thomas, A., and Schomäcker, R., *Catal. Sci. Technol.*, 2024, 14, 2114-2129.
9. Xing, F., Zeng, R., Cheng, C., Liu, Q., and Huang, C., *Appl. Catal. B: Environ. Energy*, 2022, 306, 121087.
10. Xie, L., Teng, J., Li, T., and Li, F., *J. Colloid Interface Sci.*, 2025, 679, 114-123.
11. Liu, S., Hu, Y., Huang, Y., Wang, W., Deng, P., Zhang, L., Xuan, W., and Hou, Y., *Int. J. Hydrogen Energy*, 2024, 51, 1099-1109.
12. Zhao, J., Ding, Y., Wei, J., Du, X., Yu, Y., and Han, R., *Int. J. Hydrogen Energy*, 2014, 39, 18908-18918.